Window effect in a discretized model for diffusion of a chain in one dimension

G. Terranova,[1] C. M. Aldao,[2] and H. O. Mártin[1]
[1]*Physics Department, School of Exact and Natural Sciences, University of Mar del Plata, Deán Funes 3350, 7600 Mar del Plata, Argentina*
[2]*Institute of Materials Science and Technology (INTEMA), University of Mar del Plata and National Research Council (CONICET), Juan B. Justo 4302, B7608FDQ Mar del Plata, Argentina*
(Received 19 August 2004; published 24 February 2005)

We introduce a model to study the diffusion of chains in microporous solids. The difficulties a chain has to escape from a pore where it is confined is found to strongly depend on the ratio between the chain length and the cage size. This dynamic effect implies a nonstandard behavior of the diffusion coefficient. We found a window effect that can be explained without using any energy argument.

DOI: 10.1103/PhysRevE.71.021103 PACS number(s): 05.40.Jc, 66.10.Cb, 66.30.−h, 47.55.Mh

I. INTRODUCTION

The diffusion coefficient in solids containing regular successions of cells or pores has been the subject of study for years. If the solid presents pores comparable in size to the diffusing molecules, the diffusion is strongly influenced by the interactions between molecules and walls of the solid. This diffusional regime is known as configurational, a regime in which the diffusing molecules never escape the force field of the surrounding crystal. This is the situation in the diffusion of normal paraffins in the intracrystalline space of zeolites and will be the subject of the present work [1,2].

There are many unexpected and interesting phenomena in zeolite diffusion and reaction [3–6]. In 1973 Gorring reported a phenomenon, the window effect, whereby the diffusivities of normal paraffins within zeolites *T* do not decrease monotonically with increasing carbon number *N*, as would be expected [7]. Instead, following an initial decrease with *N*, the diffusivity exhibits a local minimum followed by a pronounced local maximum. This phenomenon is one of the best-known wildly unconventional behaviors in diffusion.

The periodic nature of the diffusivity with the carbon number suggests seeking an interpretation in terms of the periodic nature of the zeolite lattice. Since the work of Gorring was reported, a number of theoretical studies aimed at explaining this experimental finding. Ruckenstein and Lee studied the diffusion of long rigid molecules in solids with successions of channels and cavities [8]. They found that diffusion presents maxima when the length of the rod is an integer of the length of the repeating structural unit of the solid and minima when it is a half integer. Later, Nitsche and Wei proposed a model in which zeolite *T* is represented by channels connected by narrower necks [9]. A linear paraffin molecule can slide along the channel and assume a number of positions, with some of the length in cells and some of the length in necks. The preferred low-energy position for a paraffin is that in which most of its length is at cells. Thus, short molecules would prefer to be completely inside a cell as the potential energy increases when the paraffin molecule penetrates a neck. For a molecule too long to fit entirely within a cell part of the paraffin will have to be at a neck. As a consequence, the difference between minimum and maximum potential energy decreases and can also be zero if the length of the molecule is an integer of the length of the repeating structural unit of the solid. More recently, Dubbeldam *et al.* were motivated to quantitatively explain the window effect with a molecular simulation method for different types of zeolites [10–12]. Simulations show that the window effect is a very generic effect that can be found in an entire class of zeolites.

In this work, we introduced a discretized model for a chain diffusing in one dimension that presents the window effect. However, differing with previous work, a window effect appears without using any energy argument but as a consequence of the entropic difficulty that a chain has to escape from a pore where it is confined.

II. MODEL

Let us consider a chain in a one-dimensional lattice consisting of *N* particles that can hop to the nearest site only if this site is empty. There can be only one particle per lattice site. Particles can hop to the right or left but no more than one site can be empty between two of them.

At each Monte Carlo step, one of the *N* particles of the chain is randomly chosen. The following situation may appear.

(i) If the selected particle is located at the end of the chain and its nearest site is occupied by another particle, the end particle jumps with probability p_a; see Fig. 1(a).

(ii) If the selected particle is located at the end of the chain and its nearest site is empty, the end particle jumps with probabilityp_b; see Fig. 1(b).

(iii) If the selected particle is not an end particle (i.e., it is a middle particle) and one of its nearest site is occupied and the other one is empty, the middle particle jumps to the empty site with probability p_c; see Figs. 1(c) and 1(d).

(iv) If the chosen selected particle is a middle particle with both nearest sites occupied, or both nearest sites empty, the middle particle does not jump and remains at its original position; see Figs. 1(e) and 1(f).

Hence, p_a, p_b, and p_c are the free parameters of the model ($0 \leqslant p_a, p_b, p_c \leqslant 1$). After each Monte Carlo step the time, *t*, is increased by $\delta t = 1/N$ so that, at a time interval equal to 1, every particle has, on average, one chance to be selected.

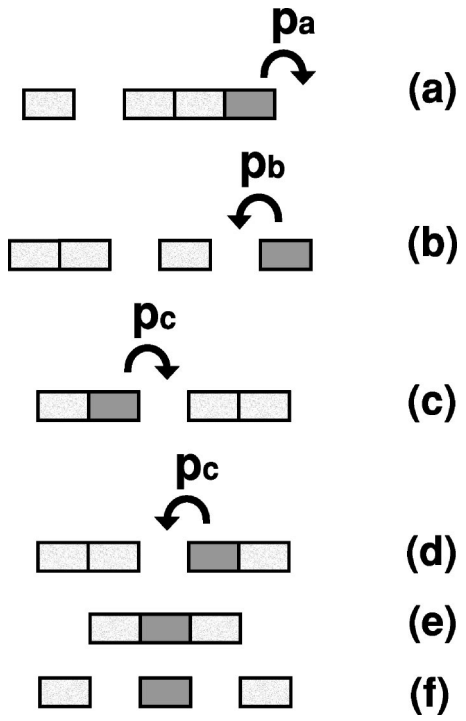

FIG. 1. Jumping probabilities for end [(a),(b)] and middle [(c),d), (e),(f)] particles. In cases (e) and (f) the middle particle, the shaded one, cannot jump.

Every time a particle jumps, the center of mass of the chain moves $1/N$ of the distance a between adjacent lattice sites. In the following we use $a=1$. The repetition of the described procedure simulates the random motion of the chain in a *free space* (i.e., without taking into account the effects of pores). This model was introduced in Ref. [13] and the properties of this free diffusion are summarized below.

In order to incorporate the porous media effect, the model is modified as follows. We add to the lattice *effective barriers* with periodicity l as shown in Fig. 2. When an end particle is adjacent to an effective barrier, rule (i) is modified such that the jumping probability adopts the value hp_a, where h $(0 \leqslant h \leqslant 1)$ is a new free parameter of the model. For $h=1$, the free diffusion case is recovered.

The simulation starts with an arbitrary chain configuration and, following the rules of the model, many jumps are performed to reach an equilibrium configuration. At this point the origin of the timescale, $t=0$, is defined. The Monte Carlo results were obtained averaging over more than 10^3 samples.

A cellular material can be envisioned as pores connected by narrow necks, as depicted in Fig. 3. These necks act diminishing the probability for end particles to jump to neighboring pores. An end particle not always finds the neck and then the chain diffusivity is reduced. Conversely, once an end particle crosses a neck, the rest of the chain can follow the leading bead. Due to the crystalline character of zeolites, necks, represented as effective barriers, are uniformely distributed.

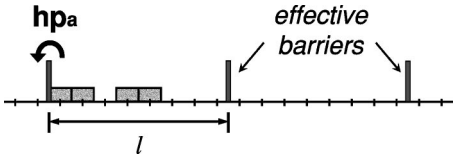

FIG. 2. Periodic effective barriers. The bars represent the effective barriers separated by a distance l. The jumping probability of the left end particle is hp_a.

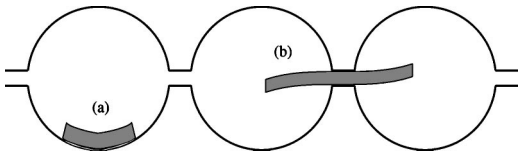

FIG. 3. Schematics showing three cells connected by necks. Molecule (a) needs to find a neck to escape from the cell that contains it. Molecule (b) diffuses freely as the neck does not include any energy interaction with the diffusing molecule.

We have introduced a one-dimensional model that resembles a three-dimensional diffusion in a porous material. Actually, the diffusing molecule describes a three-dimensional movement within the pores. Thus, a low probability for the chain end to find a neck connecting two pores is represented by the factor h in the one-dimensional model. This is equivalent to say that there are a larger number of microstates within the pore than within the neck.

We stress that the introduced effective barriers do not correspond to real energy barriers. In particular, the parameter h is not related to any energy. It reflects the difficulty that end particles have to find the channel between pores in order to move from a pore to the next one. In other words, the origin of h is due to the effects of the configurational dynamics. Clearly h plays the role of an effective parameter that takes into account, in a simple way, the complicated dynamics that a chain must perform in order to escape from a given pore where is confined. This dynamics strongly depends on the special kind of pores and chains that appear in real systems. We emphasize that the present work is focused on the understanding of a basic mechanism that produces the window effect and not to reproduce specific experimental results. Thus the proposed mechanism is described with a Monte Carlo model having a minimum of assumptions to keep it as simple as possible.

In the Monte Carlo simulation the diffusion coefficient of the chain center of mass, D, is calculated through

$$D = (\delta x_{\text{c.m.}})^2/2t, \tag{1}$$

where

$$(\delta x_{\text{c.m.}})^2 = \langle [x_{\text{c.m.}}(t) - x_{\text{c.m.}}(0)]^2 \rangle, \tag{2}$$

$x_{\text{c.m.}}$ is the position of the center of mass and the brackets denote the ensemble average.

For the case of free diffusion $(h=1)$, an analytical approximation of the diffusion coefficient can be obtained [14],

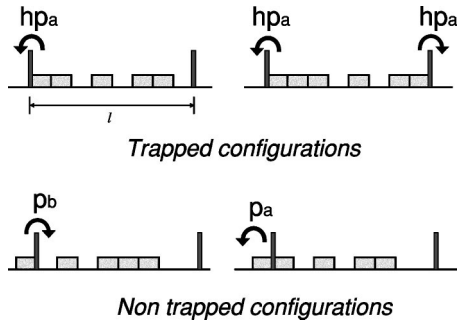

FIG. 4. Trapped and nontrapped configurations. Some examples of trapped and nontrapped chain configurations are shown.

$$D = \frac{p_a p_b p_c}{N(p_a + p_b)^2}\left(1 + \frac{2}{N}\frac{p_a + p_b - p_c}{p_c}\right). \tag{3}$$

In the limit $N \to \infty$ this approximation asymptotically converges to the exact value of D. For the special case when the relation $p_a + p_b = p_c$ holds, Eq. (3) becomes

$$D = \frac{p_a p_b p_c}{N(p_a + p_b)^2}, \tag{4}$$

which is the exact expression of D for all values of N, $N \geqslant 2$ (for more details see Ref. [14]).

We will focus now on the general case with the effective barriers present. We define as a *trapped configuration* a chain configuration in which at least one of the end particles is adjacent to an effective barrier and its nearest site is occupied (see Fig. 4). In other words, in a trapped configuration the jumping probability of one, or both ends, is hp_a. We also define the *trapped chain length* l_{tr} as the average length of the chain for trapped configurations, and the adimensional parameter $\lambda \equiv l_{tr}/l$ (i.e., the ratio between the trapped chain length and the period of the effective barriers). As it will be shown in the next section, λ is an appropriate parameter to describe the behavior of the diffusion coefficient D.

III. RESULTS AND DISCUSIONS

Let us start discussing the case $p_a + p_b = p_c$ where Eq. (4) holds. In Fig. 5 the typical behavior of the diffusion coefficient, D, as a function of the adimensional parameter λ is shown. To compare with, the Monte Carlo results of D for the free diffusion case is also plotted.

For free diffusion, D monotonously decreases as a function of N; see Eq. (4). To easily check that this is not the behavior for the case of nonfree diffusion, in Fig. 6 we plot $\delta x^2_{\text{c.m.}}$ as a function of time, t, for $N=5$, 6, 7, and 8 (and the same values of p_a, p_b, p_c, and h as those used in Fig. 5). The values of D are proportional to the slopes of the straight lines shown in Fig. 6, see Eq. (1), and then it is evident that the error bars in the values of D are much smaller than the amplitude of the oscillation shown in Fig. 5. In fact, error bars in Fig. 5 would be smaller than the symbols used.

Figure 5 clearly indicates that the chain diffusivity presents local maxima around integer values of λ. This nonstandard behavior shows the so-called *window effect* whose

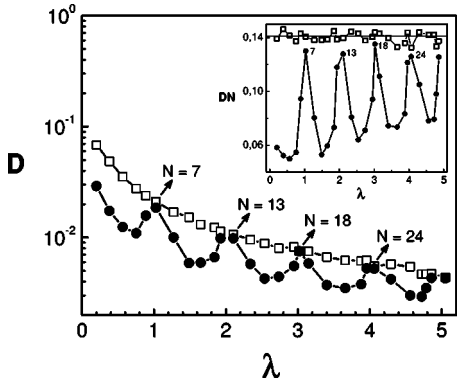

FIG. 5. The diffusion coefficient of the center of mass, D (full circles), as a function of the adimensional parameter λ. The Monte Carlo results were obtained using $p_a=0.83$, $p_b=0.17$, $p_c=1$, and $h=0.1$. For comparison D (open squares) for the free diffusion case is also plotted (i.e., $p_a=0.83$, $p_b=0.17$, $p_c=1$, and $h=1$). Since in this case λ has no meaning, D is plotted against the corresponding values of N for the nonfree diffusion case. The solid lines have been drawn to guide the eye. The inset shows the behavior of DN. The straight line corresponds to the analytical results of DN obtained from Eq. (4) for the free diffusion case.

theoretical explanation constitutes an open problem nowadays [5]. Other results, not shown in the present work, indicate that in our model the window effect is not very sensitive to the parameters p_a, p_b, and p_c, but, as expected, monotonously increases as the value of h is reduced. For example, the ratio between diffusivities corresponding to the first mamimum and the second minimum is ~ 3.2 for $h=0.1$ and ~ 15 for $h=0.01$.

In order to grasp the origin of the window effect in our model, we will analyze the chain dynamics in detail. In Fig. 7, $x_{\text{c.m.}}$ is plotted as function of time for chains with $N=4$, 7, and 10 particles. The dashed horizontal straight lines represent the position of the effective barriers ($l=10$). The values of the parameters p_a, p_b, p_c and h are the same in all cases. The values of N have been chosen in order to have three different relations between the trapped chain length, l_{tr}, and l: $l_{tr} < l$, for $N=4$; $l_{tr} \cong l$, for $N=7$; and $l < l_{tr} < 2l$, for $N=10$. Note that for long periods of time the chain with N

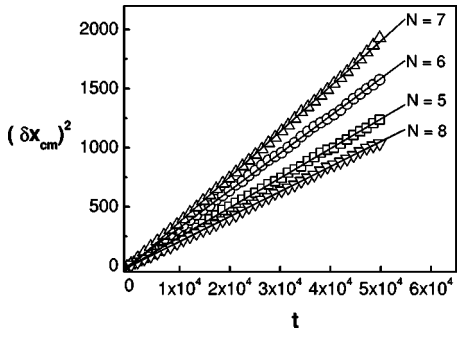

FIG. 6. The mean square displacement of the center of mass, $(\delta x_{\text{c.m.}})^2$, against time for chains of $N=5$, 6, 7, and 8 particles. The values for the parameters of the model are $p_a=0.83$, $p_b=0.17$, $p_c=1$, and $h=0.1$. The straight lines correspond to the least squares fits of the data.

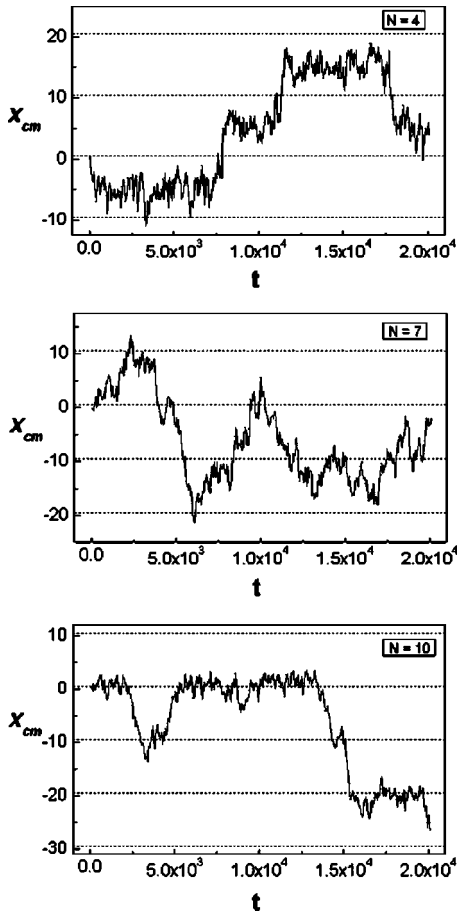

FIG. 7. Plots of the position of the center of mass, $x_{\mathrm{c.m.}}$ as function of time, t, for $p_a=0.83$, $p_b=0.17$, $p_c=1$, and $h=0.1$, $l=10$, and for chains with three different values of N: $N=4$ (a), $N=7$ (b), and $N=10$ (c). Dashed straight lines represent the positions of the effective barriers. The corresponding values of λ are $\lambda\cong 0.6$, for $N=4$ (i.e., $l_{tr}<l$); $\lambda\cong l$, for $N=7$ (i.e., $l_{tr}\cong 1$); $\lambda\cong 1.6$, for $N=10$ (i.e., $l<l_{tr}<2l$).

$=4$ appears confined between two adjacent barriers, and the chain with $N=10$ is confined between barriers separated by a distance $2l$. Interestingly, for $N=7$, $x_{\mathrm{c.m.}}$ behaves very similarly to a standard random walk (as in the case of free diffusion). That is, the presence of the effective barriers seems almost not to affect the movement of the center of mass.

For a quantitative analysis we define the *escape time*, t_{esc}, as the mean time needed for a chain to cross one of the given barriers starting from a given configuration. We say that a chain crosses a barrier if the adjacent particle to an end particle passes the barrier and both particles remain together; see Fig. 8. In the simulations we use a compressed chain (i.e., a chain with length equal to N) centered between two consecutive barriers as the initial configuration. Note that the definition of the escape time is arbitrary because there are many ways to consider when a chain crosses a barrier and to select the barrier that must be crossed. Also, other initial configurations can be chosen. However, the general conclusions are not expected to depend on the specific definition of the escape time.

In Fig. 8 we depict two possible situations in which barriers confine a chain. Confining barriers are separated by a

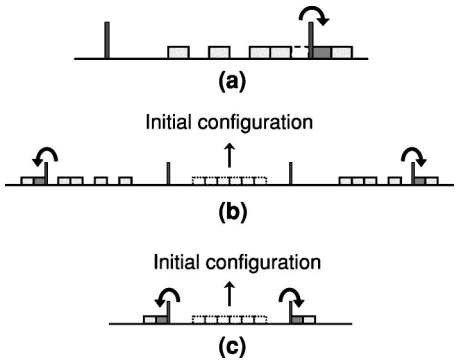

FIG. 8. Definition of the escape time, $t_{\mathrm{esc.}}$ (a) An example of a chain escaping to the right. According to our definition, the chain crosses the right barrier when the shaded particle performs the jump indicated by an arrow. In (b) and (c) two sets of confining barriers are shown. The separation between confining barriers, l_b, are $3l$ (b) and l (c). With dashed lines initial configurations are depicted. Chains escape from the corresponding confinement barriers when one of the jumping events indicated by arrows occurs. The definition of the time escape is applied for $\lambda\leqslant 3$, case (b), and $\lambda\leqslant 1$, case (c).

distance $l_b=3l$, case (b), and by a distance $l_b=l$, case (c). Case (c) can be used for $\lambda\leqslant 1$, and case (b) for $\lambda\leqslant 3$. Figure 9 shows the escape time as a function of λ using the abovementioned two sets of barriers of confinement with the same values of free parameters as those used in Fig. 5. A strong agreement between the data of Figs. 5 and 9 is clearly seen, in the sense that the local maxima in the diffusion coefficient correspond to the location of local minima in the escape times.

We will offer a qualitative explanation for the escape time dependence on the chain length for $\lambda\leqslant 1$ and $l_b=l$. It is observed that for $\lambda\sim 0.5$ the escape time is larger than for $\lambda\sim 1$ (see the inset of Fig. 9). When $\lambda\sim 1$ the chain can be confined between two consecutive barriers with both end particles being close to barriers. Thus, both end particles are very frequently trying to cross the barriers. Conversely, for shorter chains ($\lambda\sim 0.5$) only one end particle can be adjacent to a barrier. Then, since $h<1$ it is very likely for a $\lambda\sim 0.5$ chain to diffuse away from the adjacent barrier. In other

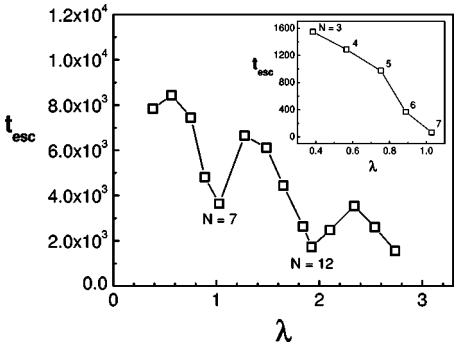

FIG. 9. The escape time, t_{esc}, as a function of λ for $l_b=3l$; see Fig. 8(b). The inset shows the behavior of t_{esc} for $l_b=l$; see Fig. 8(c). In both cases data correspond to $p_a=0.83$, $p_b=0.17$, $p_c=1$, $h=0.1$, and $l=10$. Solid lines were drawn as a guide to the eye.

words, the chain spends time moving between barriers before a successful attempt to cross a barrier takes place; see also Fig. 7(a).

For $l_b=3l$, chains with $\lambda\sim1$ or $\lambda\sim0.5$ have similar behaviors to those for $l_b=l$ (see Fig. 9) because when the chain escapes from the central barriers confinement (separated by a distance l), freely diffuses until being confined between other barriers (or it returns to the central initial position). This type of argument can be used to explain the behavior of t_{esc} for $1<\lambda<3$, shown in Fig. 9. By comparing Fig. 7(a) and the inset of Fig. 9, it seems that $x_{\mathrm{c.m.}}$ spends more time than t_{esc} to escape from being between two consecutive barriers. This implies that, after an adjacent particle to an end particle crosses a barrier, very likely the chain returns to be confined again between the same barriers.

The above reasoning can be easily extended to other values of λ. It is concluded that local minima in the escape times (and then, local maxima in the diffusion coefficient D) appear when the mean length of the trapped chains is close to a multiple integer of the barriers period.

IV. CONCLUSIONS

In previous works the window effect was explained based on particle-pore and particle-particle interactions (Refs. [8] and [9]). In contrast to the explanations presented before, we show that the window effect that we observe is not due to a net force acting on the diffusing molecule. The escape time decreases (or, equivalently, the diffusivity increases) as the length of the chain, l_{tr}, becomes equal to an integer of the distance between effective barriers. In these cases, the chain overcomes effective barriers more easily because the number of attempts per unit time becomes larger. This is another source for the appearance of the window effect, introduced with a model as simple as possible that includes only the most relevant rules.

ACKNOWLEDGMENTS

This work was partially supported by the CONICET (Argentina) and the ANPCyT (Grant No. 03-08431, Argentina).

[1] N. Y. Chen, T. F. Degman, Jr., and C. Morris Smith, *Molecular Transport and Reaction in Zeolites* (VCH, New York, 1994).
[2] J. Kärger and D. M. Ruthven, *Diffusion in Zeolites and Other Microporous Solids* (Wiley, New York, 1992).
[3] K. Hahn, J. Kärger, and V. Kukla, Phys. Rev. Lett. **76**, 2762 (1996).
[4] D. S Sholl and K. A. Fichthorn, Phys. Rev. Lett. **79**, 3569 (1997).
[5] H. Jobic, J. Kärger, and M. Bee, Phys. Rev. Lett. **82**, 4260 (1999).
[6] L. A. Clark, G. T. Ye, and R. Q. Snurr, Phys. Rev. Lett. **84**, 2893 (2000).
[7] R. L. Gorring, J. Catal. **31**, 13 (1973).
[8] E. Ruckenstein and P. S. Lee, Phys. Lett. **56A**, 423 (1976).
[9] J. M. Nitsche and J. Wei, AIChE J. **37**, 661 (1991).
[10] D. Dubbeldam, S. Calero, T. L. M. Maesen, and B. Smit, Phys. Rev. Lett. **90**, 245901 (2003).
[11] D. Dubbeldam and B. Smit, J. Phys. Chem. B **107**, 12138 (2003).
[12] D. Dubbeldam, S. Calero, T. L. M. Maesen, and B. Smit, Angew. Chem., Int. Ed. **42**, 3624 (2003).
[13] S. E. Guidoni, H. O. Mártin, and C. M. Aldao, Eur. Phys. J. E **7**, 291 (2002).
[14] S. E. Guidoni, H. O. Mártin, and C. M. Aldao, Phys. Rev. E **67**, 031804 (2003).